Green Chemistry

PAPER

View Article Online
View Journal | View Issue

Cite this: *Green Chem.*, 2014, **16**, 1316

Cleaving C–H bonds with hyperthermal H_2: facile chemistry to cross-link organic molecules under low chemical- and energy-loads†

Tomas Trebicky,[a] Patrick Crewdson,[a] Maxim Paliy,[a] Igor Bello,[a] Heng-Yong Nie,[a] Zhi Zheng,[b] Xiaoli Fan,[c] Jun Yang,[d] Elizabeth R. Gillies,[e,f] Changyu Tang,[g] Hao Liu,[g] K. W. Wong[g] and W. M. Lau*‡[g,a,e]

Received 24th July 2013,
Accepted 20th November 2013

DOI: 10.1039/c3gc41460d

www.rsc.org/greenchem

A facile method for cross-linking organic molecules has been developed by computational modeling, instrumentation design, and experimental research. Briefly, organic molecules are hit by H_2 with controllable kinetic energy in our novel apparatus where a high flux of hyperthermal H_2 is generated. When a C–H bond of the organic molecule is hit by H_2 at about 20 eV, efficient kinematic energy-transfer in the H_2→H collision facilitates the C–H dissociation with nearly 100% reaction probability. When H_2 hits other atoms which are by nature much heavier than H_2, mass disparity bars effective energy transfer and this both blocks undesirable bond dissociation and reduces unnecessary energy wastage. The recombination of the carbon radicals generated by the C–H cleavage efficiently completes the production of C–C cross-links at room temperature with no additional energy/chemicals requirements. In addition to these green chemistry merits, this new method is better than other cross-linking techniques which rely on prerequisite reactions to add cross-linkers to the organic molecules or additional reactants and additives. These promising features are validated by several cross-linking trials which demonstrate desirable mechanical, electrical, chemical, and biochemical changes while inducing no undesirable damage of chemical functionalities in the original molecules.

1. Introduction

The science of effective and selective C–H bond cleavage is fundamentally important as C–H is one of the simplest and most abundant chemical bonds found in nature. It also bears industrial relevance because many advanced functional organic materials, particularly functional polymers, comprise saturated hydrocarbon segments as their chemically inert backbones or spacers.[1] *Via* effective and selective cleavage of the C–H bonds of these materials, recombination of the carbon radicals generated by C–H cleavage can improve mechanical strength and chemical stability due to an increase of C–C cross-links. More importantly, C–C cross-links can also be exploited to graft molecules with desirable chemical groups to an inexpensive organic substrate for molecular engineering of new functional properties and applications. In reference to all known cross-linking techniques, the present work offers a new method to accomplish effective and selective C–H cleavage, with superior "greenness" derived from several unconventional reaction design considerations to reduce energy and chemical consumption, as well as increasing yield and preventing side-reactions.

The best known cross-linking method uses hydrogen abstraction with atomic hydrogen to cleave C–H bonds. However, because hydrogen abstraction typically has an energy barrier of 0.4–0.5 eV, the reaction rate becomes practical only when the temperature is raised above 300 °C.[2,3] Such sample

[a]*Surface Science Western, Western University, 999 Collip Circle, London, Ontario N6J 0J3, Canada. E-mail: llau22@uwo.ca*
[b]*Institute of Surface Micro and Nano Materials, Xuchang University, Xuchang, Henan 461000, China*
[c]*School of Materials Science and Engineering, Northwestern Polytechnical University, Xian 710072, China*
[d]*Department of Mechanical and Materials Engineering, Western University, London, Ontario N6A 5B7, Canada*
[e]*Department of Chemistry, Western University, London, Ontario N6A 5B7, Canada*
[f]*Department of Chemical and Biochemical Engineering, Western University, London, Ontario N6A 5B7, Canada*
[g]*Chengdu Green Energy and Green Manufacturing Technology R&D Center, Sichuan, 610207, China*

†Electronic supplementary information (ESI) available: Additional data to further enrich the following aspects of scientific explanation and discussion: applications of HHIC, methods and materials, estimation of C–H and C–C bond cleavage thresholds and HHIC reaction rate, and spectroscopic data. See DOI: 10.1039/c3gc41460d

‡Present address: Chengdu Science and Technology Development Center – Green Energy and Green Manufacturing Technology R&D Center, Chengdu, Sichuan 610207, China.

heating is not desirable because at this elevated temperature many organic molecules lose their chemical functionalities and polymeric solids deform or decompose. In addition, driving reactions merely with thermal energy generally violates the principles of green chemistry, as when thermal energy is used to overcome the activation energy barrier of the reaction of a specific chemical functional group, it is also consumed by the translational/rotational/vibrational excitation of all chemical moieties in the reaction environment.

Although thermal energy consumption can be reduced by adopting ultraviolet irradiation, electron/ion irradiation, plasma exposure, and other radical-mediated reactions to break C–H bonds and induce molecular cross-linking,[4] most chemical functional groups will also be altered or destroyed by such treatment methods with limited chemical selectivity. Some of these techniques also induce undesirable reactions deep below the substrate surface and cause damage to the bulk properties. In the context of controlling surface grafting reactions with surgical precision, various surface-initiated polymerization methods[5] including atom transfer radical polymerization[6] have been developed along with other preparative reactions to cleave C–H bonds and add a desirable chemical functional group onto the carbon site. However, these processes typically involve multiple steps and consume considerable amounts of reactive chemicals, heat, and time.[5] In parallel to further research and development along this path, some other techniques promising precise C–H cleavage have also been reported recently, and these include special collision-induced dissociation,[2,3,7–10] metal-mediated dissociation,[11] or even site-specific charge-injection/extraction by scanning tunnelling microscopy.[12,13] Again, they are not cost-effective or scalable, and no practical applications of these methods have been exploited in manufacturing.

Herein, we report on a facile, inexpensive, and scalable method to effectively and preferentially break C–H bonds. A schematic description of this method is sketched in Fig. 1.

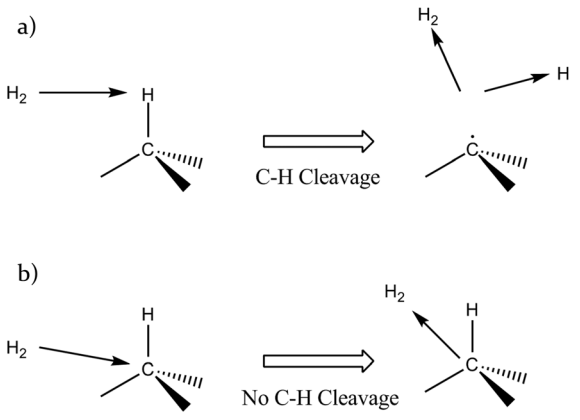

Fig. 1 Schematics of C–H cleavage as induced by hyperthermal H_2. (a) H_2 hitting H of a C–H bond, possessing enough kinetic energy to break the bond and knocking H off of the molecule; (b) H_2 hitting C of a C–H bond, ineffectively transferring some of its kinetic energy to the methane molecule and bouncing off of it.

Briefly, the selective bond cleavage reaction is designed using H_2 as a light-mass projectile with a controllable kinetic energy of ~20 eV to knock off the hydrogen atoms of C–H bonds. With both computational and experimental results, we demonstrate that the kinematic energy-transfer (meaning energy transfer imposed by kinematics) under this collision condition is only effective when the projectile impacts upon a hydrogen atom due to closely matching masses of the projectile–target pair ($H_2 \rightarrow H$). In this case, the C–H cleavage is preferential and chemical selectivity is accomplished. The only chemical reagent in this peculiar C–H cleavage process is a small amount of molecular H_2, which is chemically inert enough not to drive any other reactions. In addition to high selectivity, chemical reactivity is also high because in the present hyperthermal low-energy regime, the collision probability[14] of H_2 hitting a hydrogen atom of the C–H bonds present in the molecular layer of hydrocarbon-based organic matter is so high that the projectile H_2 will not penetrate the first few molecular layers with no collision; therefore, C–H cleavage by hyperthermal H_2 is highly effective.

To present the new method, we first use our *ab initio* molecular dynamics simulations to lay down the basic physics and chemistry of collision-induced dissociation of C–H bonds by hyperthermal H_2. We then compare this unconventional reaction design with other relevant and known methods for collision-induced dissociation of C–H. After establishing the novel chemistry, we show the practicality of the method by explaining our design of a novel process and apparatus for inexpensively generating a high flux of hyperthermal H_2. The scalability of the process and equipment for practical production is also examined. Finally, we show several practical examples to illustrate how this method can be exploited to cross-link organic matter with molecular control-precision.

2. Methods and materials

2.1. Basic physics and chemistry of cleaving C–H bonds with hyperthermal H_2

The basic concept of preferentially cleaving C–H bonds with hyperthermal[15] H_2 is depicted in Fig. 1 and validated with our *ab initio* molecular dynamics simulations shown in Fig. 2, with the relevant molecular motions shown in Video S1 and other detailed descriptions included in the ESI.† In essence, the underlying physics and novelty in this reaction design is collision-induced dissociation of C–H without breaking other bonds. This is an unconventional reaction pathway which does not require thermal energy to overcome the reaction barrier, yet offers high reactivity and high chemical selectivity. With the help of molecular-dynamic modeling, we found that when hyperthermal H_2 with ~20 eV in kinetic energy collides with C_2H_6, a hydrogen atom can be excised from C_2H_6 through a mechanism close to direct recoiling[16,17] (Fig. 1 and 2). In summary, the computational results for the $H_2 \rightarrow C_2H_6$ collision confirm the following details of collision-induced dissociation of C–H by hyperthermal H_2:

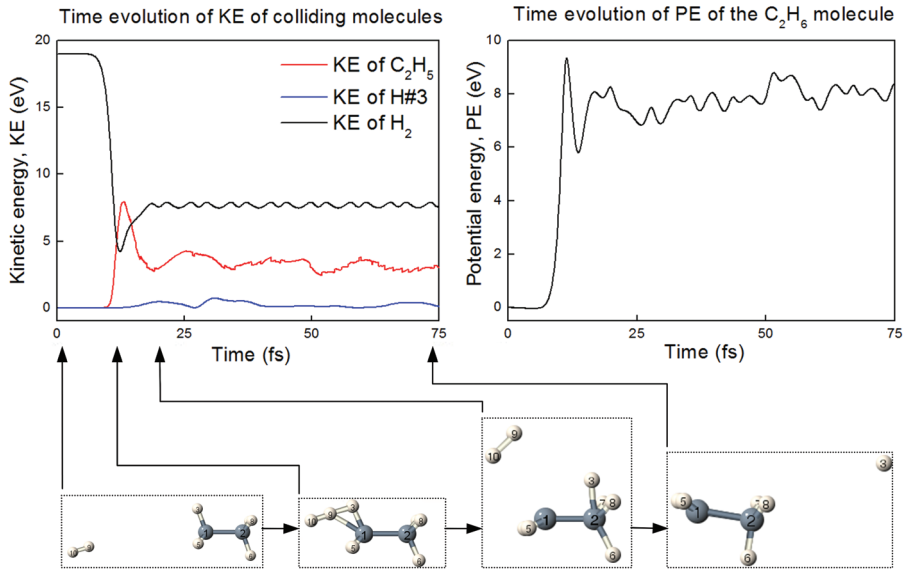

Fig. 2 Computational results of *ab initio* molecular dynamics showing cleavage of the C–H bond of C_2H_6 by 19 eV H_2 with the molecular axis of H_2 perpendicularly aligned with that of a H–C bond of C_2H_6 (note: the respective views of $H_{\#4}$ and $H_{\#7}$ of C_2H_6 are blocked by $H_{\#5}$ and $H_{\#8}$).

• When H_2 (comprising $H_{\#9}$ and $H_{\#10}$ in Fig. 2, at 19 eV in translational energy) hits $H_{\#3}$ of C_2H_6 with the molecular axis of the H_2 projectile perpendicular to the bond axis of H–C of C_2H_6, as shown in Fig. 2, $H_{\#3}$ receives enough kinematic energy-transfer from the H_2 projectile to overcome the chemical potential of the $H_{\#3}$–$C_{\#1}$ bond and thereby leaves $C_{\#1}$. The recoiled $H_{\#3}$ is held for a few femto-seconds by the $C_{\#2}$ bonding site of C_2H_5, before its departure from the recoiled C_2H_5, as shown in Video S1 of the ESI†. The analysis of the reaction dynamics of $H_{\#3}$ clearly shows a recoil-like mechanism of collision-induced dissociation. On the other hand, the analysis also shows the nature of many-body interactions, as the reaction dynamics involves all atoms and their highly correlated motions. More precisely speaking, the recoil-like mechanism is different from the ideal binary H_2→H collision during which a hard sphere with an atomic mass of 2 hits another hard sphere with an atomic mass of 1. For example, our molecular dynamics analysis shows that the H_2 projectile retains 8 eV in translational energy after its head-on collision of $H_{\#3}$ of C_2H_6. In comparison, in the framework of the ideal binary hard-sphere collision of H_2→H, the projectile H_2 after a head-on collision should only retain 2 eV in translational energy. The discrepancy mainly arises from the fact that $H_{\#3}$ of C_2H_6 is not an unconstrained H atom but a chemical constituent of C_2H_6 in the form of a covalent H–C bond. In this analysis context, we note the interesting fact that the collision of Ne→Cu with Ne impacting a copper crystal at 20 eV is known[18] to behave like a binary hard-sphere collision. Hence, *ab initio* molecular dynamics simulations play an important role in our work on designing and engineering hyperthermal H_2 induced C–H cleavage, as well as clarifying its scientific contents.

• Our simulations also show that while the scattered H_2 retains 8 eV in translational energy, the recoiled C_2H_5 gains a translational energy of ~3 eV. In comparison, the recoiled $H_{\#3}$ carries less than 1 eV in translational energy. Most of the loss of the initial impact energy (19–8–3–1 eV = ~8 eV) is consumed by the bond-cleavage energy and the internal energy of the recoiled C_2H_5.

• A small amount (<1 eV) of the initial impact energy is converted to vibrational energy of the scattered H_2. Similarly, in the context of transferring translational energy to vibrational energy during collision, a previous study[14] shows that in the event of H^+→H_2 collision at 20 eV, the relative probability of exciting H_2 from the vibrational state of 0→1 is merely 8.5%, and that of 0→2 is 3.6%. Hence, the associated energy loss during collision does not play a dominant role in our present work. This supports the effectiveness of hyperthermal H_2 being an effective recoiling agent under the conditions of our method.

In the present study, we have examined over 50 different collision trajectories and confirmed that hyperthermal H_2 induced C–H cleavage indeed follows a recoil-like mechanism constrained mainly by collision kinematics. In addition, when the projectile hits the carbon atom of C_2H_6, the ethane target remains intact for H_2 projectiles with kinetic energies below 39 eV (Fig. S1†), supporting our hypothesis that there exists an ineffective energy transfer regime in H_2→C collisions. The threshold energy for C–C cleavage was found to be 40 eV. This leads to a practical and wide kinetic energy window of 20–40 eV for preferential C–H cleavage with good energy efficiency.

The main working principle of our proposed method is the mass matching of the projectile (H_2) and the desirable colliding atomic-site (H of a C–H bond). As expected, we indeed found from our computational and experimental results that when H_2 is replaced by any heavier projectile such as He, the selectivity for preferentially breaking C–H bonds is lost. This is because heavier projectiles can no longer effectively

differentiate hydrogen atoms from other target atoms by their mass and the mass-dependent kinematics (as detailed in the ESI).†

Although the computational results shown in Fig. 2 suggest a threshold H_2 energy of ~20 eV for cleaving C–H in C_2H_6, the threshold is expected to drop when the C–H bond is part of a saturated hydrocarbon segment of a macroscopic solid. It is because only a negligible amount of the incident energy is lost to the translational kinetic energy of the solid. In contrast, such transfer does occur in an isolated C_2H_6 molecule, as shown above. Additional discussion and estimation of both (C–H and C–C) thresholds is included in the ESI.†

2.2. Comparative analysis of the novelty of using hyperthermal H_2 to cleave C–H

The use of hyperthermal H_2 as the projectile of choice in our experiments is novel in several aspects. First, although the recoiling mechanism has been adopted in direct recoiling spectrometry in which helium and other inert gases with a typical kinetic energy of 1–100 keV are used to knock off atoms from a sample for chemical compositional analysis,[16] target atoms are recoiled indiscriminately without any chemical selectivity. For example, Rodriguez *et al.* used 4–6 keV Ar^+ as a projectile to recoil H, C, S, Ga, and As atoms from an alkyl-thiol target on Au(111) in order to reveal the adsorption dynamics of the system.[17] In comparison, we have successfully used our hyperthermal H_2 collision method to preferentially cleave C–H bonds of an alkyl self-assembled-monolayer and to cross-link these molecules either as nano-clusters or as a two-dimensional molecular layer without losing any of the constituent atoms other than hydrogen.

The novelty of the hyperthermal H_2 collision method is also evident when compared to the collision-induced dissociation mechanisms discovered earlier by Ceyer[19] regarding the breaking of C–H bonds of CH_4 physisorbed on Ni(111). Ceyer showed that when CH_4 physisorbed on Ni(111) is hit by a hyperthermal argon atom, the projectile transfers some energy to CH_4 and is backscattered, with a mechanism similar to binary hard-sphere collision. The subsequent forward motion of the CH_4 leads to its deformation and induces the conversion from physisorption to dissociative chemisorption. Ceyer also showed that by replacing argon with krypton, which is much heavier than CH_4, the krypton atom after a collision is not backscattered but moves forward with CH_4. This leads to hammering CH_4 into the Ni substrate and results in dissociative chemisorption. Although both cases yield C–H cleavage, they are fundamentally different from our method in that Ceyer's mechanisms of C–H cleavage do not yield the recoiling of a hydrogen atom by the incident projectile. In fact, if the Ceyer's mechanisms are applied to organic molecules more complex than CH_4, C–H cleavage will be accompanied by the cleavage of other bonds and preferential C–H cleavage cannot be accomplished. In fact, our molecular dynamics simulations indeed show such problems when inert gas atoms such as He and Ar are used to collide with organic molecules. In all cases, undesirable side reactions of other bond cleavages and yield-reduction of C–H cleavage are observed.

The present method of using hyperthermal H_2 as an agent of C–H cleavage is a breakthrough from our previous work,[8–10] where we employed H^+ to break C–H bonds. In these previous studies we took advantage of the availability of a low energy mass-separated ion beam system in our research laboratory to precisely control the kinetic energy of H^+ ranging from 2.0 ± 0.6 eV to 100.0 ± 0.6 eV in order to prove collision-induced selective C–H cleavage and its energy dependence. Although the scientific results nicely support the reaction model shown in Fig. 1, this ion-beam method is not practical because most organic materials are electrically insulating and have surface charging problems when exposed to ionized species such as H^+. Further, the generation and transport of a high flux of hyperthermal H^+ is technically challenging because low-energy ions travel relatively slowly and are subject to strong space-charge repulsion. This results in beam-spreading which seriously limits the flux density and the reaction throughput; this means that although a set of collision-induced dissociation experiments can be carried out, the experimental time is impractically long. In addition, H^+ is chemically reactive and may drive undesirable side-reactions, including halogen abstraction and carbonyl reduction. By replacing H^+ with the chemically more inert and neutral H_2, we resolve these shortcomings of H^+.

2.3. Engineering design of a high flux of hyperthermal H_2

To take full advantage of the novel chemistry of selectively cleaving C–H with hyperthermal H_2, we must first overcome the relevant technical difficulties in generating a high flux of hyperthermal H_2. In this context, the known method of generating a supersonic molecular beam[20,21] typically gives hyperthermal H_2 with a kinetic energy and beam current too low for practical selective C–H cleavage. The method of neutralizing a hyperthermal H_2^+ beam[22] is also impractical because of its flux limitation due to space-charge-induced spreading of a low energy ion beam as explained earlier. Although collision processes involving H_2 have been studied for many decades,[2,3,8–10,14–16,20–26] these studies have never explored methods for the generation of a high flux of hyperthermal H_2 to treat a practically large sample-area. More specifically, the instrumentation goal in our work on making hyperthermal H_2 induced C–H cleavage practical is to build an inexpensive apparatus to generate a flux density of 10^{16} cm^{-2} of H_2 at ~20 eV per second uniformly covering a sample area of 100 cm^2. With such an apparatus, surface engineering of a large sample of 100 cm^2 with our new method of hyperthermal H_2 induced C–H cleavage is fast and can be completed within a few seconds. Industrial applications can be further exploited by adding a roll-to-roll sample-feedthrough to the apparatus, to take advantage of the fast rate of the new C–H cleavage method.

In Fig. 3 we show the basic apparatus design in compliance with the above instrumentation specifications. Briefly, an intense beam of hydrogen ions is extracted from an electron

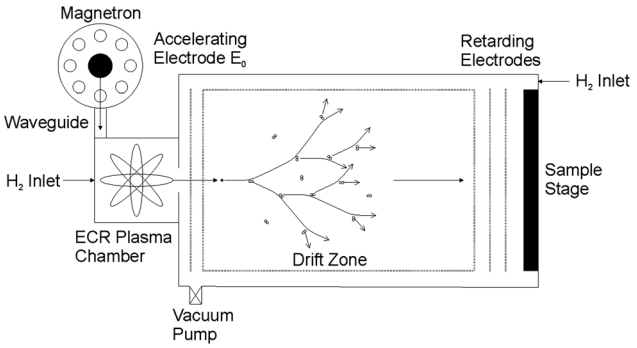

Fig. 3 Schematic diagram of the HHIC reactor.

cyclotron resonance microwave plasma[27] which is widely used in industry for plasma-assisted deposition and etching. The ions are accelerated to an appropriate kinetic energy (300–400 eV) with an applied electric field and fed into a long drift tube (about 50 cm in length) filled with H_2 to a pressure around 1 mTorr (0.13 Pa). At the pressure of 1 mTorr, each H_2 molecule will likely collide with another H_2 molecule every time it travels 10 cm. Under this condition, every hydrogen ion coming out from the ion source will collide with an H_2 molecule in the drift tube, transfer its energy effectively to its collision partner due to mass matching, and initiate a cascade of collisions in the drift tube. The cascade collisions in the drift tube generate and deliver a high flux of hyperthermal H_2 at the end of the drift tube where a sample is placed. Additional grid electrodes on top of the sample holder are used, with appropriate voltage biases, to repel ions and electrons present near the end exit of the drift tube.

To explore the technical details of this design, we used a Monte Carlo (MC) technique to simulate the cascade of collisions. Fig. 4a provides snap-shots from such MC simulations (details are shown in the ESI,† with collision motions shown in Video S2). The MC simulations predicted yields of hyperthermal H_2 projectiles as a function of the H_2 pressure in the drift zone and the energy of H_2 at the drift-zone exit, which are shown in Fig. 4b. The results indicate that there is an optimal pressure where the yield reaches a maximum. For example, the best yield of H_2 projectiles capable of breaking C–H bonds can be found near a H_2 pressure of ~1 mTorr (0.13 Pa) for 400 eV H^+ entering a drift zone of 50 cm in length.

2.4. Experimental processes of hyperthermal hydrogen induced cross-linking

The prototype apparatus shown in Fig. 3 was used to study selective C–H cleavage and subsequent molecular cross-linking by carbon radical recombination. This combined process is referred to as hyperthermal hydrogen induced cross-linking (HHIC). When a microwave power of 300 W was used, an HHIC sample treatment typically took less than a minute for a sample treatment area of ~500 cm^2. The cascade collision process for generating a high flux of hyperthermal H_2 was facilitated by extracting the ions from the ECR H_2 plasma with

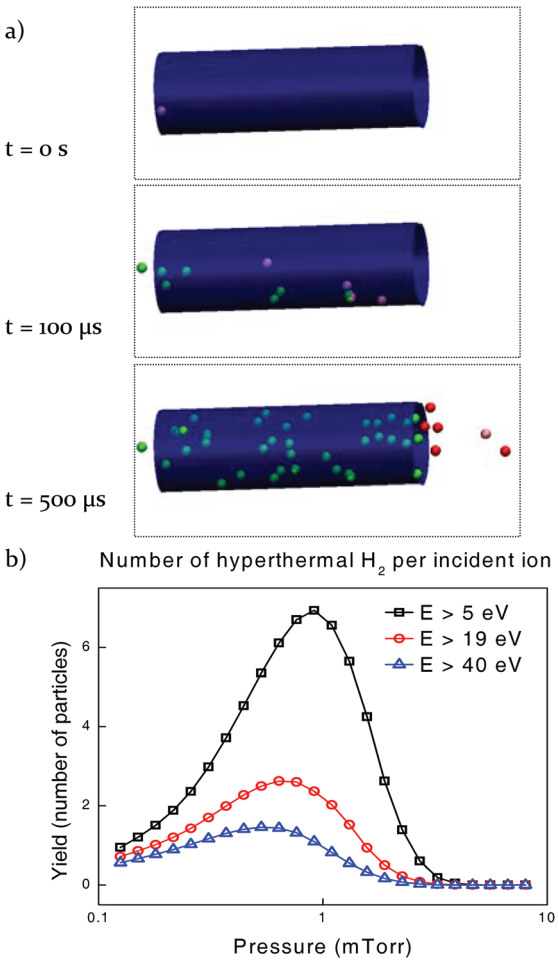

Fig. 4 (a) Monte Carlo simulations of time evolution of a gas-phase (293 K, 1 mTorr) cascade of collisions in a drift zone (blue tube) initiated by 400 eV H^+ projectile. The H_2 projectiles with energies E > 5 eV are shown in red, those with E < 5 eV are shown in green, and the background gas particles not participating in the collision cascade are not shown; (b) the yield of H_2 projectiles per incident particle.

a voltage of 200–400 V. With a microwave power of 300 W, the total ion extraction current was ~0.1–0.2 A; hence, the power consumption for ion extraction was <100 W. The energy consumption increases when the microwave power is raised to generate a higher ion flux, but this also leads to a higher flux of hyperthermal H_2 and thus a reduction of the HHIC treatment time. Such a high throughput condition can be realized by rushing samples through the reactor with a roll-to-roll sample feeder.

2.5. Energy consumption of the HHIC process

The fast throughput condition is desirable in reducing the overall HHIC energy consumption per unit-area of sample-treatment because in addition to microwave energy consumption and other throughput-dependent energy consumption factors, the HHIC process also has throughput-independent power consumption and this fixed-overhead consumption makes the average energy consumption per unit-area sample

treatment high when the throughput is slow. The following energy cost factors are fixed-overhead consumption: electromagnet to generate a local magnet field of 0.0875 T for the maintenance of the ECR condition; and the vacuum operation tools to keep a hydrogen pressure of 1 mTorr. On the whole, when such a high throughput condition is adopted, the HHIC process complies well with the principles of green engineering: (a) it operates at room temperature; (b) reaction activation barrier of C–H cleavage is overcome by depositing energy preferentially to the C–H bonds; (c) only H_2 is used to facilitate the process and it is not consumed by the cross-linking reaction; and (d) the process is engineered to prevent side-reactions.

3. Results and discussion

3.1. Experimental validation of HHIC

To validate the cross-linking effects of HHIC, we deposited a thin layer of dotriacontane (n-$C_{32}H_{66}$) onto freshly cleaved mica and used the surface sensitive technique of X-ray photoelectron spectroscopy (XPS) to monitor the layer thickness. In this experiment, when the exposure of the layer to hyperthermal H_2 was not sufficient, the layer was removed by a simple heptane rinse due to inadequate cross-linking. With an increased exposure to hyperthermal H_2, the degree of cross-linking was raised which reduced the layer solubility and led to an efficient retention of the layer thickness. Using the thickness as a metric allowed us to study the dependence of the degree of cross-linking on the hydrogen ion extraction energy. The dependence is summarized in Fig. 5. As expected, the HHIC effectiveness drops when the hydrogen ion extraction energy is too low, as not enough H_2 projectiles having sufficient energy to break C–H bonds are produced.

The efficiency of HHIC, in reference to the throughput of the cross-linking reaction, is another important figure of merit. From the computational results like those shown in Fig. 4b, we estimate that the typical total fluence (number of particles per unit area) of useful hyperthermal H_2 arriving at the sample surface is $\sim 7 \times 10^{15}$ cm^{-2}. Assuming that at least 2 C–H bonds per $C_{32}H_{66}$ molecule must be cleaved in order to cross-link all $C_{32}H_{66}$ units into an insoluble film, we estimate that the rate constant of C–H cleavage by HHIC is at least $\sim 10^{-11}$ cm^3 per molecule per second (details are given in the ESI†). This is approximately 9 orders of magnitude more effective than C–H cleavage by hydrogen abstraction using atomic hydrogen.[3,28] Moreover, cross-linking a 10 nm thin film of dotriacontane *via* HHIC, *i.e.* rendering it insoluble, takes only a few seconds. Hence, the reaction throughput is high enough for HHIC to be used in a roll-to-roll production of molecular films.

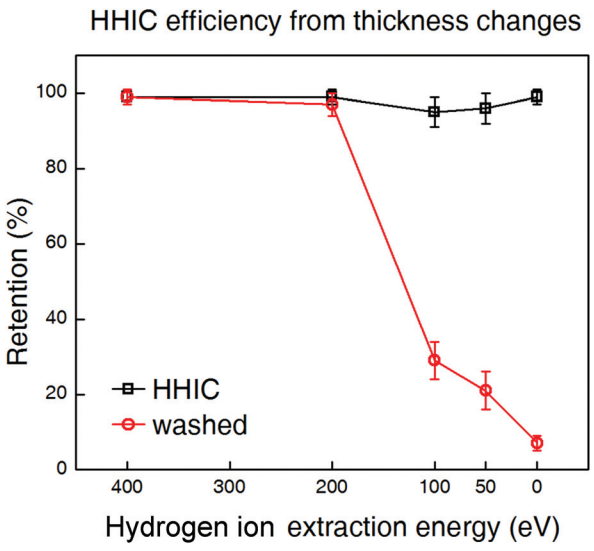

Fig. 5 Effectiveness of C–H cleavage of n-$C_{32}H_{66}$ as a function of hydrogen ion extraction energy, showing a drastic reduction of cross-linking efficiency for projectiles having insufficient energy to cleave C–H bonds. Shown is the retention of sample thickness after HHIC (labelled "HHIC") and after washing (labelled "washed").

3.2. Practical applications of the HHIC technology

Three examples are shown in Fig. 6–8 and other relevant applications recently reported in the literature are cited to illustrate the feasibility and versatility of the HHIC technology.

3.2.1. Engineering mechanical strength. In engineering functional polymers and organic materials, an increase in surface mechanical strengths without changing the bulk elastic properties can lead to an enhancement of the durability, reliability and life-time of many products. In principle, this engineering requirement can be satisfied by increasing the density of C–C cross-links in the near-surface region of the polymer or organic substrate. But, accomplishing this without comprising other physical and chemical properties of the bulk substrate is not trivial. Here, we demonstrate that with the

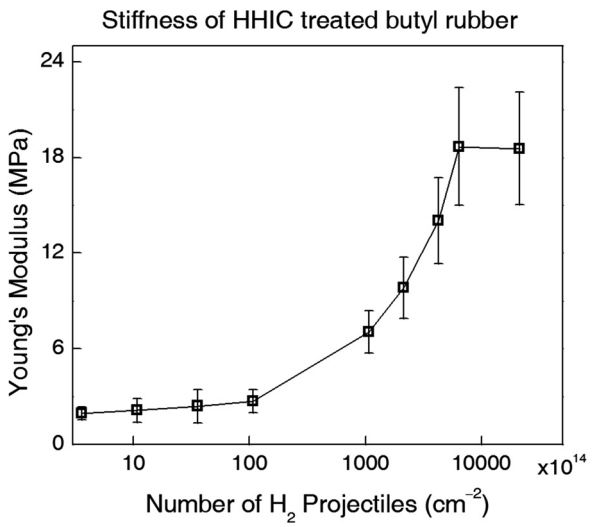

Fig. 6 Engineering of surface mechanical properties of butyl rubber.

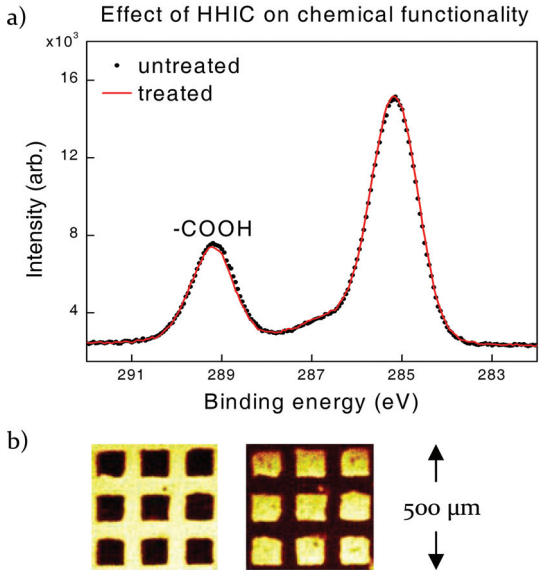

Fig. 7 (a) Untreated and HHIC treated PAA showing over 96% retention of COOH functionality as shown by XPS; (b) negative ToF-SIMS ion images of patterned PAA; left: Si substrate (SiO_3H^- signal); right: cross-linked PAA (C_6H^-).

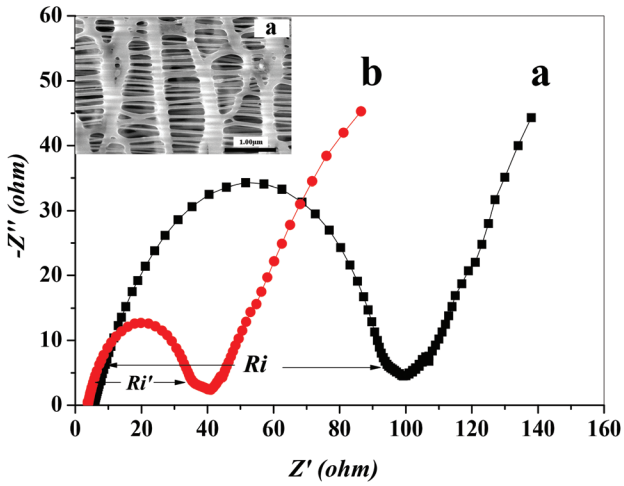

Fig. 8 A.C. impedance spectra of a lithium-ion cell assembled by sandwiching (a) pristine separator and (b) PEO-coated separator treated by HHIC after chloroform washing for 12 h; the inset shows the microstructure of the separator which remained intact before and after the HHIC treatment.

HHIC technique, we can drastically increase the Young's modulus at the surface of an elastomer. In this trial demonstration, we used butyl rubber as a model elastomer substrate and treated it with HHIC under different treatment conditions. After each HHIC treatment, we employed spectroscopic analyses such as FTIR and XPS to confirm the retention of the hydrocarbon nature of the surface chemistry with no addition of any chemical functional groups. Young's modulus in the surface region of about 10 nm in depth was measured with an atomic force microscope. Fig. 6 summarizes the changes in surface Young's modulus as a function of hyperthermal H_2 fluence. In essence, a brief HHIC treatment of 30 seconds for the generation of hyperthermal H_2 with a moderate microwave power of 300 W using the HHIC apparatus design shown in Fig. 3 is sufficient to cause a 20-fold increase in surface mechanical strength. A scale-up version of this design can thus be used to produce such surface-engineered elastomer sheets with an inexpensive and fast throughput rate of production. Such facile and drastic changes of surface mechanical properties of a polymer with a simple collision-induced dissociation reaction like HHIC have never been reported.

3.2.2. Examples of engineering pure surface functionality. In this set of examples, we demonstrate the merit of HHIC in engineering surface chemistry. The quest focuses specifically on premium surface engineering products which require a set of precisely controlled chemical functional groups and cannot tolerate any significant amounts of chemical contaminants. In this demonstration trial, we chose to use polypropylene to model any simple and inexpensive saturated polymer substrate which is known to be a difficult substrate for chemical grafting.

In the first example, we chose to anchor and cross-link a hydrophilic molecular layer of poly(acrylic acid) (PAA) onto the hydrophobic polypropylene substrate. This surface engineering task was planned to show that simple spin-casting a PAA solution on polypropylene, with a subsequent brief HHIC process to cross-link the deposited PAA, can form a stable molecular layer with the highest density of carboxylic acid functional group among all known materials (one COOH per two carbon atoms on a hydrocarbon chain). Fig. 7a shows the XPS evidence that virtually no acrylic acid groups were damaged by this HHIC process. By comparison, only ~73% of the acrylic acid groups were preserved and some contaminating oxygen-containing functionalities were introduced when the best plasma polymerization process to date was used to cross-link PAA.[29] The stability of the HHIC-cross-linked PAA layer was also confirmed by its insolubility in common solvents which are effective in dissolving untreated PAA. This example demonstrates the important and unique merit of the HHIC process: virtually perfect preservation of desirable chemical functionality in the process of cross-linking the hydrocarbon backbones, a merit which guarantees the features of green chemistry including high product yield, no side products, and low chemicals consumption and wastes. This merit is also a key to opening the lock blocking the demands of cross-linking/grafting results offering a set of pure chemical functionality, particularly for premium electronic or biomedical applications. In addition to this merit, Fig. 7b displays selective area patterning accomplished through shadow-masking in conjunction with the HHIC treatment yielding cross-linked and insoluble PAA. The pattern transfer is applicable to the production of novel chemical, biomedical, and electronic sensors and other electronic devices such as field-effect transistors.

The second example of HHIC's applicability in engineering pure chemical functionality is about improving a lithium-ion

battery by modifying its separator membrane which is placed in the electrolyte of the battery to separate the anode and cathode. In the current field, polypropylene membranes with the microstructure shown in the inset of Fig. 8 are the most commonly used separators. Our hypothesis is that we can raise the electrolyte wettability and reduce the internal resistance of the battery by grafting polyethylene oxide (PEO) to polypropylene with HHIC. Briefly, our HHIC experiment indeed yielded the stable anchoring of PEO onto the polypropylene separator membrane with no change of the membrane microstructure shown in Fig. 8. The PEO functionality was confirmed with FTIR and XPS. Before the HHIC treatment, the pristine separator had a water contact angle of 108° and the contact angle corresponding to the electrolyte solvent (mixture of EC and DMC) was 59°; after the HHIC treatment, the respective contact angles were reduced to 27° and 34°. The results show that indeed the HHIC treatment of grafting and cross-linking PEO on a polypropylene separator can improve its wetting ability.

In order to evaluate the surface modification effect of the separator on the electrochemical properties, we prepared half-cells having the structure of $LiCoO_2$/separator/lithium metal and characterized them with standard AC impedance spectroscopy. The results are summarized in Fig. 8. Briefly, the overlapping semicircles correspond to the charge accumulation process and charge transfer process, both of which are critically affected by the impedance of the electrolyte–separator interface. From these data, the changes in the interface impedance can be tracked and measured. As shown in Fig. 8, the interface impedance of the pristine separator was 100 Ω and the impedance dropped to 40 Ω when the separator was modified with cross-linked PEO by HHIC. This trial has already been expanded into an engineering project to optimize the charging/discharging properties and reliability of lithium-ion batteries.

In addition to these original data demonstrating the applicability of HHIC, some other HHIC's applications[30,31] were reported recently. For example, HHIC was also used to covalently bond PEO onto a butyl rubber substrate.[30] Most importantly, this work shows that the outstanding PEO nature of anti-protein adsorption was transfused to the butyl rubber substrate. The adsorption of fibrinogen, a common protein, was drastically reduced by the PEO HHIC treatment, as confirmed by fluorescent microscopy which is sensitive to the detection of fibrinogen.[31] In another recently known application of HHIC, physisorbed poly(2-(dimethylamino)ethyl methacrylate) (PDMAEMA) onto a substrate having C–H bonds with no undesirable change of the original chemical functionality,[32] which is similar to the fixation of PAA with no damage of its carboxylic functionality. The cross-linked PDMAEMA was then quaternized to form the final product—an antimicrobial film. In comparison to the conventional method of surface-initiated atom transfer radical polymerization for accomplishing the same antimicrobial effect,[33] this HHIC-based method[32] consumes much less chemical reagents and is much less costly.

4. Conclusion

In conclusion, we have demonstrated an effective way to use hyperthermal H_2 to cleave C–H bonds selectively. Obeying the basic principle of kinematic energy-transfer, the light-mass projectile differentiates its colliding partners by their atomic mass. Like the scalpel of a skilful surgeon, it only excises hydrogen from a C–H bond while leaving other bonds intact. This novel method allowed us to perform a wide range of

Table 1 Green chemistry contents of HHIC

Principle of green chemistry	Green chemistry contents of HHIC
Energy should be minimized	Cleaving a C–H bond always requires energy. In HHIC, a clever way is developed for depositing energy specifically to the H atom of a C–H bond to cleave the bond. More importantly, the method minimizes the deposition of energy to other atoms in the chemical process system. In comparison, most current methods for cleaving C–H bonds deposit energy indiscriminatingly to all components in the chemical process system. Hence, HHIC is relatively energy efficient.
Synthetic method should be conducted at room temperature	Most current methods for cleaving C–H bonds require a processing temperature higher than room temperature. HHIC is conducted at room temperature.
Waste should be prevented	HHIC aims at preferential cleavage of C–H with no undesirable bond cleavages. This approach prevents waste and formation of side-products.
Chemical products should be designed to preserve efficacy of function	In HHIC, molecules are cross-linked with the preservation of their functional chemical groups.
Synthetic methods should be designed to maximize the incorporation of all materials used in the process into the final product	HHIC has a very high reaction probability and yet low probability of side-reactions. As such, it is designed to maximize the incorporation of all materials used in the process into the final product.
Use of auxiliary substances (solvents, separation agents, *etc.*) should be made unnecessary	HHIC does not require any auxiliary substances.
Unnecessary derivatization should be avoided	Unlike many C–H cleaving and cross-linking methods, HHIC does not require any derivatization steps.

practical applications in the fields of chemistry, molecular engineering, and organic electronics for which no other single technique could have produced similar results. Furthermore, the manufacturing cost is low because the reactor is relatively simple and consumes no reactive gases other than a small amount of H_2, and the effective generation of a high flux of hyperthermal H_2 allows the processing of large samples at a high throughput of a few seconds per sample with no thermal energy requirement. On the whole, the novel process gives a near-perfect example of reaction design using the principles of green chemistry, as shown in Table 1.

Author contributions

W. M. Lau and Z. Zheng conceived and designed the hyperthermal proton method for selective C–H cleavage. X. L. Fan and M. Paliy did the computational work. I. Bello, T. Trebicky, and W. M. Lau designed and built the HHIC reactor. W. M. Lau, J. Yang, E. R. Gillies, C. Y. Tang, H. Liu, and K. W. Wong conceived and designed the HHIC applications in polymer engineering. T. Trebicky, P. Crewdson, and C. Y. Tang conducted the HHIC experiments. J. Yang and H. Y. Nie conceived and designed the work on measuring Young's modulus changes with atomic force microscopy. T. Trebicky and H. Y. Nie conceived, designed, and conducted the work with time-of-flight secondary ion mass spectrometry. W. M. Lau, T. Trebicky, M. Paliy, P. Crewdson, C. Y. Tang, H. Liu, and K. W. Wong led the manuscript preparation and revision.

Competing interest

The authors declare no competing financial interest.

Acknowledgements

This work was made possible by the facilities of the Shared Hierarchical Academic Research Computing Network (SHARCNET: http://www.sharcnet.ca) and Compute/Calcul Canada, Surface Science Western, Chengdu Science and Technology Development Center, and Chengdu Green Energy and Green Manufacturing Technology R&D Center. This work was supported by the Natural Science and Engineering Research Council in Canada, Ontario Centres of Excellence, the Ontario Ministry of Research and Innovation, the Beijing Computational Science Research Center, the National High Technology Research and Development Program (863 Program # 2013AA050905) in China, and the CAEP Grant 2013B0302058 in China.

References

1 C. Pugh and A. L. Kiste, *Prog. Polym. Sci.*, 1997, **22**, 601–691.
2 W. Q. Zhang, Y. Zhou, G. R. Wu, Y. P. Lu, H. L. Pan, B. N. Fu, Q. A. Shuai, L. Liu, S. Liu, L. L. Zhang, B. Jiang, D. X. Dai, S. Y. Lee, Z. Xie, B. J. Braams, J. M. Bowman, M. A. Collins, D. H. Zhang and X. M. Yang, *Proc. Natl. Acad. Sci. U. S. A.*, 2010, **107**, 12782–12875.
3 B. N. Kerkeni and D. C. Clary, *Phys. Chem. Chem. Phys.*, 2006, **8**, 917–925.
4 F. Garbassi, M. Morra and E. Occhiello, *Polymer surfaces from physics to technology*, Wiley, Chichester, New York, 1994.
5 S. Edmondson, V. L. Osborne and W. T. S. Huck, *Chem. Soc. Rev.*, 2004, **33**, 14–22.
6 T. E. Patten, J. H. Xia, T. Abernathy and K. Matyjaszewski, *Science*, 1996, **272**, 866–868.
7 W. Q. Zhang, H. Kawamata and K. P. Liu, *Science*, 2009, **325**, 303–306.
8 Z. Zheng, X. D. Xu, X. L. Fan, W. M. Lau and R. W. M. Kwok, *J. Am. Chem. Soc.*, 2004, **126**, 12336–12342.
9 Z. Zheng, R. W. M. Kwok and W. M. Lau, *Chem. Commun.*, 2006, 3122–3124.
10 Z. Zheng, K. W. Wong, W. C. Lau, R. W. M. Kwok and W. M. Lau, *Chem.–Eur. J.*, 2007, **13**, 3187–3192.
11 W. H. Bernskoetter, C. K. Schauer, K. I. Goldberg and M. Brookhart, *Science*, 2009, **326**, 553–556.
12 A. D. Zhao, Q. X. Li, L. Chen, H. J. Xiang, W. H. Wang, S. Pan, B. Wang, X. D. Xiao, J. L. Yang, J. G. Hou and Q. S. Zhu, *Science*, 2005, **309**, 1542–1544.
13 S. Katano, Y. Kim, M. Hori, M. Trenary and M. Kawai, *Science*, 2007, **316**, 1883–1886.
14 S. Amaran and S. Kumar, *J. Chem. Phys.*, 2007, **127**, 214304.
15 D. C. Jacobs, *Annu. Rev. Phys. Chem.*, 2002, **53**, 379–407.
16 J. W. Rabalais, *Science*, 1990, **250**, 521–527.
17 L. M. Rodriguez, J. E. Gayone, E. A. Sanchez, O. Grizzi, B. Blum, R. C. Salvarezza, L. Xi and W. M. Lau, *J. Am. Chem. Soc.*, 2007, **129**, 7807–7813.
18 L. L. Tongson and C. B. Cooper, *Surf. Sci.*, 1975, **52**, 263–269.
19 S. T. Ceyer, *Science*, 1990, **249**, 133–139.
20 R. D. Levine, *Molecular reaction dynamics*, Cambridge University Press, Cambridge, UK, New York, 2005.
21 G. Scoles, *Atomic and molecular beam methods*, Oxford University Press, New York, 1988.
22 J. H. Rechtien, R. Harder, G. Herrmann, A. Nesbitt, K. Tellioglu and K. J. Snowdon, *Surf. Sci.*, 1993, **282**, 137–151.
23 D. Troya and G. C. Schatz, *Int. Rev. Phys. Chem.*, 2004, **23**, 341–373.
24 K. Sakimoto, *J. Chem. Phys.*, 2000, **112**, 5044–5053.
25 S. C. Althorpe, F. Fernandez-Alonso, B. D. Bean, J. D. Ayers, A. E. Pomerantz, R. N. Zare and E. Wrede, *Nature*, 2002, **416**, 67–70.
26 L. F. Errea, C. Illescas, A. Macias, L. Mendez, B. Pons, I. Rabadan and A. Riera, *J. Phys. B: At., Mol. Opt. Phys.*, 2009, **42**, 125027.
27 T. Taylor and J. S. C. Wills, *Nucl. Instrum. Methods Phys. Res., Sect. A*, 1991, **309**, 37–42.

28 T. C. Sandreczki and I. M. Brown, *Macromolecules*, 1990, **23**, 1979–1983.
29 J. Friedrich, R. Mix, G. Kuhn, I. Retzko, A. Schonhals and W. Unger, *Compos. Interface*, 2003, **10**, 173–223.
30 C. V. Bonduelle, W. M. Lau and E. R. Gillies, *ACS Appl. Mater. Interfaces*, 2011, **3**, 1740–1748.
31 A. Halperin, *Langmuir*, 1999, **15**, 2525–2533.
32 S. Karamdoust, B. Y. Yu, C. V. Bonduelle, Y. Liu, G. Davidson, G. Stojcevic, J. Yang, W. M. Lau and E. R. Gillies, *J. Mater. Chem.*, 2012, **22**, 4881–4889.
33 J. Y. Huang, H. Murata, R. R. Koepsel, A. J. Russell and K. Matyjaszewski, *Biomacromolecules*, 2007, **8**, 1396–1399.